Desalination and Water Treatment
www.deswater.com

doi: 10.5004/dwt.2017.20660

77 (2017) 19–29
May

Comparison of performance and economics of reverse osmosis, membrane distillation, and pressure retarded osmosis hybrid systems

Yongjun Choi[a], Seung-Hyun Kim[b], Sangho Lee[a,*]

[a]*School of Civil and Environmental Engineering, Kookmin University, Jeongneung-Dong, Seongbuk-Gu, Seoul 136-702, Korea, Tel. +82-2-910-4529; Fax: +82-2-910-4939; email: sanghlee@kookmin.ac.kr (S. Lee)*
[b]*School of Civil Engineering, Kyungnam University, Woryeong-dong, Masanhappo-gu, Changwon-si, Gyeongsangnam-do 631-701, Korea*

Received 6 October 2016; Accepted 21 November 2016

ABSTRACT

This paper intended to evaluate the performance and economics of hybrid desalination systems including reverse osmosis (RO) stand-alone, RO–membrane distillation (MD), RO–pressure retarded osmosis (PRO), and RO–MD–PRO. Theoretical analysis for evaluating the performance of hybrid systems was carried out using previously validated RO, MD, and PRO numerical models. Moreover, a simple cost model was applied to analyze the effects of seawater total dissolved solids, energy cost, membrane cost, and interest rate. Results showed that the hybrid systems can outperform an RO stand-alone system in terms of its ability to reduce water cost and alleviate the disposal and environmental problems of waste brine. The electricity cost plays a dominant role in determining economic feasibility of hybrid plants. The steam cost for MD heating source plays a dominant role in determining economic feasibility of RO–MD and RO–MD–PRO hybrid systems. The membrane cost and interest rate are also crucial factors affecting the economic feasibility of hybrid systems.

Keywords: Reverse osmosis; Membrane distillation; Pressure retarded osmosis; Hybrid desalination; Economic analysis

1. Introduction

Water scarcity is becoming a critical issue for sustainable development in many countries all over the world. More than 1.2 billion people lack access to clean drinking water [1] and the number is expected to continuously increase. Since the freshwater resource is limited, saline water desalination technologies have drawn attention as one of the most promising methods to solve the water scarcity problem [2]. Over the past few decades, several desalination technologies have been developed, including thermal distillation (multi-stage flash distillation, multi-effect distillation, and mechanical vapor pressure compression distillation), membrane separation (reverse osmosis [RO] and nanofiltration), freezing, and electrodialysis [3]. Among them, RO is one of the most dominant technologies in the seawater desalination market since it has the lowest geographical restrictions as well as is a proven, reliable, and established process [4,5]. According to the International Desalination Association, for 2011, RO was used in 66% of installed desalination capacity (44.5 of 67.4 mm^3/d). Nevertheless, RO technology also has drawbacks such as high electricity consumption and low recovery ratio of product water [6]. The energy consumption for RO desalination systems lies between 2.5 and 4.0 kWh/m^3 depending on many parameters (i.e., intake type, pretreatment, seawater salinity, etc.) [3]. The recovery ratio of product water of desalination by RO systems is in the range of 30%–40% [3].

Typical costs of water desalination by RO is in the range of 0.5–1.0 USD/m^3, which has been achieved by advances in energy recovery devices and membranes with improved performance; however, a decrease in costs due to technological developments is not foreseen as energy costs will increase [3,7]. At the same time, brine discharge regulations are getting more stringent, raising the costs for new projects [8].

* Corresponding author.

As a response to these issues, hybrid desalination systems based on RO are those employing novel membrane processes such as membrane distillation (MD), pressure retarded osmosis (PRO), and forward osmosis (FO). In particular, a combination of RO, MD, and PRO is thought to be a favorable candidate to improve recovery ratio of product water and brine water quality, reduce the water cost.

MD is a separation process using a vapor pressure, which results from the temperature difference between feed and permeate water [9]. The hydrophobic micro-porous membrane facilitates the transport of water vapor through its pores, while maintaining vapor–liquid interfaces at the pore entrance, but it does not participate in the actual separation process. MD has several advantages compared with RO and other desalination processes for the treatment of saline water [10–12]. Because water is transported through the membrane only in a vapor phase, MD can offer complete rejection of all non-volatile constituents in the feed solution; thus, almost 100% rejection of ions, dissolved non-volatile organics, colloids, and pathogenic micro-organisms can be achieved via the MD process. But more importantly, due to the discontinuity of the liquid phase across the membrane, water flux in MD is not influenced by the osmotic pressure gradient across the membrane. Consequently, the greatest potential of MD can be realized through the treatment of highly saline solutions [10].

PRO is a variant of FO in which a pressurized concentrated draw stream and a more dilute feed stream are separated by a semi-permeable membrane, so that the permeate from the feed can enter the draw stream in a pressurized state from which useful power may be extracted [13]. Investigations into PRO have resumed over the last decade due to advances in membrane technology, and have received considerable attention as a salinity gradient power process [14]. PRO is mostly regarded as an environmentally friendly and sustainable energy production process that uses seawater or concentrated seawater (i.e., brine from desalination system) as the draw solution, while river water or wastewater effluent is used as the feed solution [15,16].

Although the interest in hybrid desalination technologies is growing, little information is available on their performances and economic aspects. Accordingly, this paper focused on the economic analysis of RO stand-alone, RO–MD, RO–PRO, and RO–MD–PRO hybrid systems. Evaluation of the performance of hybrid systems was carried out using previously validated RO, MD, and PRO numerical models. A cost analysis model was applied to examine the effects of seawater total dissolved solids (TDS), energy cost, membrane cost, and interest rate on the RO and hybrid systems.

2. Materials and methods

2.1. Hybrid systems

RO and three proposed hybrid configurations were considered as shown in Fig. 1. These configurations were determined by considering the sequence of each system and the influent concentration. In the RO–MD hybrid system, seawater flows into the RO membrane as a feedwater preferentially and then the RO brine is used as the MD feed solution in order to achieve higher recovery of water. In the RO–PRO hybrid system, the brine from the RO process is used as a draw solution for the PRO process without additional pretreatment, and pretreated effluent from a wastewater treatment plant is used as the feed solution for the PRO process to produce higher osmotic power and alleviate the disposal and environmental problems of waste RO brine. In the RO–MD–PRO hybrid system, first the RO brine is used as the MD feed solution and then MD brine is used as a draw solution for the PRO process without additional pretreatment, and pretreated effluent from a wastewater treatment plant is used as the feed solution for the PRO process.

2.2. RO model

The solution–diffusion model modified with the film theory model was applied to analyze the performance of RO process. For an RO process, the water flux (J_w) and solute flux (J_s) equations can be defined as follows [17]:

$$J_w = A(P - \Delta\pi_{C_{F,m}} - P_{\text{loss}}) \tag{1}$$

$$J_s = B(C_{F,m} - C_p) \tag{2}$$

where A is the water transport coefficient, B is the salt transport coefficient, $C_{F,m}$ is the salt concentration on the membrane surface, C_p is the salt concentration at the permeate side, $\Delta\pi_{C_{F,m}}$ is the osmotic pressure, P is the feed pressure, and P_{loss} is the pressure drop in the module.

$$P_{\text{loss}} = \frac{k_f 12\mu u L}{H^2} \tag{3}$$

where k_f is the friction coefficient for the channel wall and spacers, μ is the dynamic viscosity of feedwater, H is the feed channel height, L is the feed channel length, and u is the cross-flow velocity of the feedwater.

The osmotic pressure is directly related to the concentration of each solution with the modified van't Hoff formula:

$$\pi = \frac{NRT}{M_w} C \tag{4}$$

where N is ionization number in the water, R is the ideal gas constant, T is the temperature, M_w is the molecular weight, and C is the salt concentration.

$C_{F,m}$ is calculated according to the film theory to interpret the concentration polarization, and the solvent concentration profile on the surface can be calculated according to the following equation [17]:

$$\frac{C_{F,m} - C_p}{C_{F,b} - C_p} = e^{\frac{J_w}{k}} \tag{5}$$

where $C_{F,b}$ is the salt concentration in the feed bulk solution and k is the mass transfer coefficient for the back diffusion

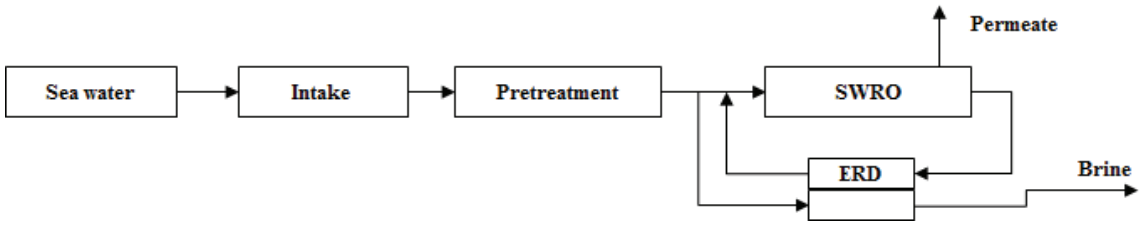

a) RO system

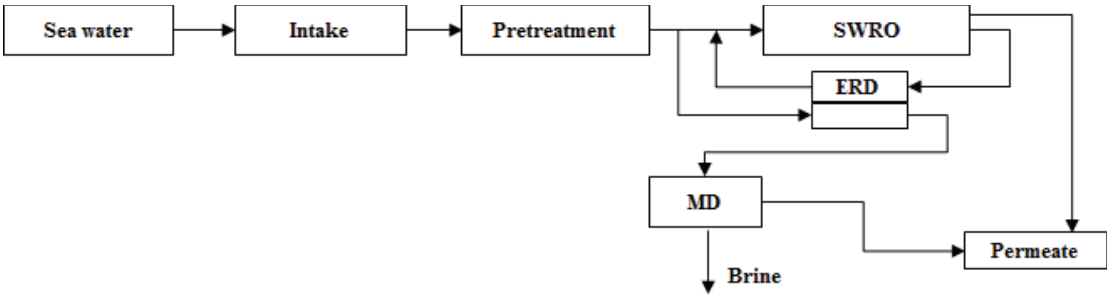

b) RO-MD hybrid process

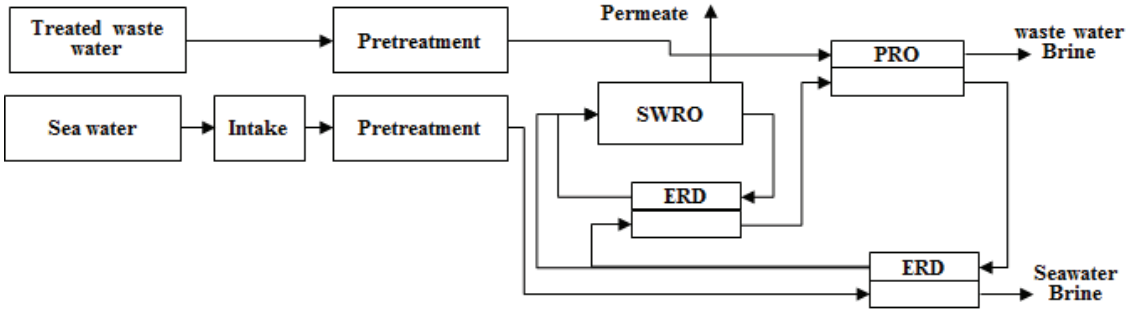

c) RO-PRO hybrid process

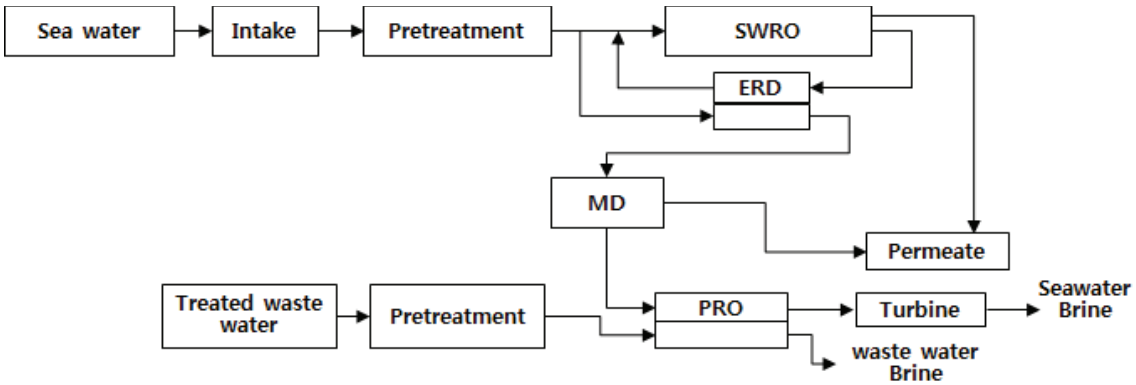

d) RO-MD-PRO process

Fig. 1. Schematic of (a) RO stand-alone system, (b) RO–MD, (c) RO–PRO, and (d) RO–MD–PRO hybrid systems.

of the solute from the membrane to the bulk solution on the high-pressure side of the membrane [17] as follows:

$$k = \frac{ShD}{d_h} \tag{6}$$

$$Sh = 1.85\left(\mathrm{Re}\,Sc\frac{d_h}{L}\right)^{0.33} \quad \left(Re \le 2100\right) \tag{7}$$

$$Sh = 0.04\,\mathrm{Re}^{0.75}\,Sc^{0.33} \quad \left(Re > 2100\right) \tag{8}$$

where D is the diffusion coefficient, d_h is the hydraulic diameter, Sh is the Sherwood number, Re is the Reynolds number, and Sc is the Schmidt number.

2.3. MD model

MD process has four different configurations, including direct contact MD, air gap MD, sweeping gas MD, and vacuum MD (VMD). Among them, the VMD configuration was selected in this study. In the VMD process, the driving force is maintained by applying a continuous vacuum at the permeate side below the equilibrium vapor pressure. The hot feed solution is brought into contact with one side of a hydrophobic micro-porous membrane. In the case of mass transport of water through the membrane, the water vapor flux, J_w is expressed as follows [9,18,19]:

$$J_w = A_B[P_v(T_m, C_m) - P_0] \tag{9}$$

where A_B is the VMD coefficient of the membrane, T_m is the temperature on the membrane surface in the feed side, C_m is the concentration on the membrane surface in the feed side, $P_v(T_m, C_m)$ is the water vapor pressure on the membrane surface in the feed side, and P_0 is the pressure in the vacuum side.

The water vapor pressure on the membrane surface in the feed side may be related with the temperature and feed solution concentration. The vapor pressure, $P_v(T_m, C_m)$ is expressed as follows [20]:

$$P_v(T_m, C_m) = \frac{\exp\left(aT_m^{-1} + bT_m + cT_m^{2} + dT_m^{3} + e\log(T_m)\right)}{1 + 0.57257\left(\dfrac{C_m}{1000 - C_m}\right)}$$

$$a = -5.80 \times 10^{3} \tag{10}$$
$$b = 1.39 - 4.86 \times 10^{-2}$$
$$c = 4.18 \times 10^{-3}$$
$$d = -1.45 \times 10^{-8}$$
$$e = 6.55$$

C_m is calculated according to the film theory to interpret the concentration polarization, and the solvent concentration profile on the surface can be calculated according to the following equation [17]:

$$\frac{C_m}{C_b} = \exp\left(\frac{J_w}{k}\right) \tag{11}$$

where C_b is the concentration in the feed bulk solution and k is the mass transfer coefficient for the back diffusion of the solute from the membrane to the bulk solution. The mass transfer coefficient, k can be calculated same as RO.

In a general MD process, the mass transfer may be explained, in principle based on, different possibilities: the Knudsen flow model, the viscous flow model, the molecular diffusion model, or a combination of them [9,19–23]. In a VMD configuration, the molecular diffusion model may not be an adequate representation of mass transfer in view of the low partial pressure of air inside the pores. Thus, the mass transport mechanisms through hydrophobic micro-porous membrane in VMD could either be a Knudsen flow model or viscous flow model or a combination of both [23]. The average pore diameter of the MD membrane is commonly smaller than the mean free path of water vapor. Hence, the Knudsen flow model is adopted by the majority of mass transport mechanisms in VMD configuration [23]. In the Knudsen flow model, A_B is expressed as follows [23]:

$$A_B = \frac{MD^{kn}}{RT_m\delta} \tag{12}$$

$$D^{kn} = \frac{2\varepsilon r}{3\tau}\left(\frac{8RT_m}{\pi M}\right)^{0.5} \tag{13}$$

where M is the water molecular mass, D_{kn} is the Knudsen diffusion coefficient, R is the gas constant, δ is the membrane thickness, ε is the porosity, r is the pore size, and τ is the pore tortuosity. MD involves mass transfer of water vapor coupled with heat transfer across the membrane. Heat transfer across the membrane boundary layer in an MD system is a limiting step for mass transfer. This is because a large quantity of heat must be applied to the vapor–liquid interface to vaporize the liquid. In an MD system, heat transfer occurs through latent heat transfer that accompanies the vapor flux and conduction heat transfer across the membrane [9]. Consequently, there is a rather complex relationship between heat and mass transfer. This problem is related and involved with the presence of an unstirred boundary layer that adjoins the membrane. This implies that the temperature at the membrane surface, T_m, is lower than the corresponding value at the well-stirred bulk phase, T_b. The phenomenon is called temperature polarization and masks the real magnitude of the driving force [9]. In a VMD configuration, however, the conductive heat across the membrane is negligible due to the low pressure on the permeate side of the membrane [9]. Hence, the heat flux through the liquid boundary layer can be represented with the following equation [23]:

$$h_w(T_m - T_b) = J_w\Delta H_v \tag{14}$$

where ΔH_v is the latent heat of vaporization, h_w is the heat transfer coefficient, T_b is the feed bulk temperature, and

T_m is the temperature in membrane surface. The heat transfer coefficient is calculated in similar way to the mass transfer coefficient [23].

$$h_w = \frac{K_m Nu}{dh} \tag{15}$$

$$Nu = 1.86\left(\mathrm{Re}\cdot\mathrm{Pr}\cdot\frac{dh}{L}\right)^{0.33} \quad \left(Re \le 2100\right) \tag{16}$$

$$Nu = 0.023\,\mathrm{Re}^{0.8}\,\mathrm{Pr}^{0.33} \quad \left(Re > 2100\right) \tag{17}$$

2.4. PRO model

In the PRO process, the water and salt flux is limited by external concentration polarization (ECP) due to the stagnant layers caused by reduced mixing on the membrane surface and internal concentration polarization (ICP) due to resistance against salt transport in the porous support layer [13,14]. Therefore, water flux (J_w) and salt flux (J_s) equations for PRO can be defined as follows [13,14]:

$$J_w = A\left(\pi_{D,m} - \pi_{F,m} - P\right) \tag{18}$$

$$J_s = B\left(C_{D,m} - C_{F,m}\right) \tag{19}$$

where $\pi_{D,m}$ and $C_{D,m}$ are the osmotic pressure and salt concentration of draw water on the membrane surface, $\pi_{F,m}$ and $C_{F,m}$ are the osmotic pressure and salt concentration of feedwater in the membrane support layer. $C_{D,m}$ and $C_{F,m}$ are expressed as followings [13,14]:

$$C_{D,m} = \left[C_{D,b}\exp\left(-\frac{J_w}{k}\right)\right] \tag{20}$$

$$C_{F,m} = \left[C_{D,m} - \frac{C_{D,m} - C_{F,b}\exp\left(KJ_w\right)}{1 + \frac{B}{J_w}\left[\exp(KJ_w) - 1\right]}\right] \tag{21}$$

where K and k are the mass transfer resistance for ICP and mass transfer coefficient for ECP, respectively.

Using $C_{D,m}$ and $C_{F,m}$ instate of $C_{D,b}$ and $C_{F,b}$, the water flux (J_w) and salt flux (J_s) equations can be modified as follows:

$$J_w = A\left(\frac{N_D RT_D}{M_{w,D}}C_{D,b}\exp\left(-\frac{J_w}{k}\right) - \frac{N_F RT_F}{M_{w,F}}\left(C_{D,m} - \frac{C_{D,m} - C_{F,b}\exp\left(KJ_w\right)}{1 + \frac{B}{J_w}\left[\exp(KJ_w) - 1\right]}\right) - P_s\right) \tag{22}$$

$$J_s = B\left(C_{D,b}\exp\left(-\frac{J_w}{k}\right) - C_{D,m} - \frac{C_{D,m} - C_{F,b}\exp\left(KJ_w\right)}{1 + \frac{B}{J_w}\left[\exp(KJ_w) - 1\right]}\right) \tag{23}$$

where P_s is the pressure of draw water of PRO process.

The power density W of the PRO membrane module was calculated using the product of J_w and P_s [21]:

$$PD = J_w P_s \tag{24}$$

2.5. Cost model

In order to analyze the effects of major parameters such as seawater TDS, membrane cost, energy cost, interest rate, and steam cost for VMD heat source on RO, RO–MD, RO–PRO, and RO–MD–PRO systems, a set of cost functions were used [24–29]. Based on these cost function, a theoretical model was developed to evaluate the economics of RO, MD, and RO–MD hybrid system.

- Intake:

$$CC_{IT}[\$] = 598 \times (Q_f[m^3/d]/0.9)^{0.78} \tag{25}$$

$$OC_{IT}[\$/d] = 0.028 P_{IT}[bar] Q_f[m^3/d]/0.9 \times D_{eng}[\$/kWh]/\eta_{P\_IT} \times PLF \tag{26}$$

- Pretreatment:

$$CC_{\mathrm{Pre}}[\$] = 400 \times 0.7 \times (Q_f[m^3/d]/0.9)^{0.78} \tag{27}$$

$$OC_{\mathrm{Pre}}[\$/d] = 0.028 P_{\mathrm{Pre}}[\mathrm{bar}] Q_f[m^3/d]/0.9 \times D_{\mathrm{eng}}[\$/\mathrm{kWh}]/\eta_{P\_\mathrm{Pre}} \times \mathrm{PLF} \tag{28}$$

- High-pressure pump:

$$CC_{\mathrm{HP}}[\$] = Q_f[m^3/d](393{,}000 + 10{,}710 P_{f,\mathrm{in}}[\mathrm{bar}]) \tag{29}$$

$$OC_{\mathrm{HP}}[\$/d] = 0.028 P_{\mathrm{f,in}}[\mathrm{bar}] Q_f[m^3/d] D_{\mathrm{eng}}[\$/\mathrm{kWh}]/\eta_{P\_HP} \times \mathrm{PLF} \tag{30}$$

- Booster pump:

$$CC_{\mathrm{BP}}[\$] = (Q_f[m^3/d] - Q_p[m^3/d])(393{,}000 + 10{,}710(P_{f,\mathrm{in}}[\mathrm{bar}] - P_{f,\mathrm{out}}[\mathrm{bar}]\eta_{\mathrm{ERD}}) \tag{31}$$

$$OC_{\mathrm{BP}}[\$/d] = \frac{(0.028(P_{\mathrm{f,in}} - P_{\mathrm{f,out}})[\mathrm{bar}]\eta_{\mathrm{ERD}}(Q_f - Q_p)[m^3/d] D_{\mathrm{eng}}[\$/\mathrm{kWh}])}{\eta_{P\_BP}} \times \mathrm{PLF} \tag{32}$$

- Energy recovery device:

$$CC_{\mathrm{ERD}}[\$] = (Q_f[m^3/d] - Q_p[m^3/d])(393{,}000 + 1.07P_{f,\mathrm{in}}[\mathrm{bar}])/2 \quad (33)$$

- Vacuum pressure pump:

$$CC_{\mathrm{VP}}[\$] = \frac{Q_f[m^3/d](393{,}000 + 10{,}710))}{12{,}000P_{\mathrm{VP}}[\mathrm{mbar}]} \quad (34)$$

$$OC_{\mathrm{VP}}[\$/d] = 1.0\left[\frac{\mathrm{kWh}}{m^3}\right]Q_p[m^3/d]D_{\mathrm{eng}}[\$/\mathrm{kWh}] \times \mathrm{PLF} \quad (35)$$

- Heat exchanger:

$$CC_{\mathrm{HX}}[\$] = 1000 \times \mathrm{Area}_{HX} \quad (36)$$

- Turbine:

$$CC_{\mathrm{Tur}}[\$] = (Q_f[m^3/d]])(393{,}000 + 1.07P_{f,\mathrm{out}}[\mathrm{bar}])/5 \quad (37)$$

- Steam:

$$OC_{\mathrm{Steam}}[\$/d] = (\mathrm{Steam[kg/day]} \times C_{\mathrm{Steam}}[\$/\mathrm{kg}]) \quad (38)$$

where CC and OC denote the capital cost and operating cost. P and η are pressure and efficiency. The subscripts, IT, Pre, HP, BP, ERD, VP, HX, and Tur denote the intake, pretreatment, high-pressure pump, booster pump, energy recovery device, vacuum pressure pump, heat exchanger, and turbine. Q_f and Q_p is the feed and permeate flow rate, respectively. D_{eng} is the unit electricity cost, C_{steam} is the unit steam price, and PLF is the plant load factor. Assuming that the capital cost of the membrane is linear to the membrane area, the annualized capital cost of the membrane is calculated by the following equation [26–28]:

$$CC_{\mathrm{Mem}}[\$] = \mathrm{Area}_{\mathrm{Mem}}C_{\mathrm{mem}}[\$/m^2] \quad (39)$$

where the subscript Mem denotes the membrane, $Area_{\mathrm{Mem}}$ is the total membrane area, and C_{mem} is the unit membrane cost.

The total capital cost is composed of the direct capital cost and the indirect capital cost. The direct capital cost is the sum of the cost for plant equipment and the cost for site development, which is set at 10% of equipment cost [17]. The indirect capital cost is set at 20% of the direct capital cost. The total and annual capital costs of hybrid process are expressed as follows [25–27].

- RO process:

$$CC_{\mathrm{Equipment}}[\$] = CC_{IT} + CC_{\mathrm{Pre}} + CC_{HP} + CC_{BP} + CC_{\mathrm{Mem}} \quad (40)$$

- RO–MD hybrid system:

$$CC_{\mathrm{Equipment}}[\$] = CC_{IT} + CC_{\mathrm{Pre}} + CC_{HP} + CC_{BP} + CC_{\mathrm{Mem}} + CC_{VP} + CC_{HX} \quad (41)$$

- RO–PRO hybrid system:

$$CC_{\mathrm{Equipment}}[\$] = CC_{IT} + CC_{\mathrm{Pre}} + CC_{HP} + CC_{BP} + CC_{\mathrm{Mem}} + CC_{\mathrm{TUR}} \quad (42)$$

- RO–MD–PRO hybrid system:

$$CC_{\mathrm{Equipment}}[\$] = CC_{IT} + CC_{\mathrm{Pre}} + CC_{HP} + CC_{BP} + CC_{\mathrm{Mem}} + CC_{VP} + CC_{HX} + CC_{\mathrm{Tur}} \quad (43)$$

$$CC_{\mathrm{Site}}[\$] = CC_{\mathrm{Equipment}} \times 0.2 \quad (44)$$

$$DCC[\$] = CC_{\mathrm{Equipment}} + CC_{\mathrm{Site}} \quad (45)$$

$$\mathrm{ICC}[\$] = \mathrm{DCC} \times 0.3 \quad (46)$$

$$\mathrm{TCC}[\$] = \mathrm{DCC} + \mathrm{ICC} \quad (47)$$

$$\mathrm{ACC}[\$/y] = \mathrm{TCC}\frac{i(1+i)^n}{(1+i)^n - 1} \quad (48)$$

The annual operating cost is composed of the annual power cost, annual membrane replacement cost, and other cost (labors, chemicals, and maintenance). The annual operating costs of hybrid processes are expressed as follows [25–27].

- RO system:

$$OC_{\mathrm{Power}}[\$/y] = (OC_{IT} + OC_{\mathrm{Pre}} + OC_{HP} + OC_{BP}) \times 365 \quad (49)$$

- RO–MD system:

$$OC_{\mathrm{Power}}[\$/y] = (OC_{IT} + OC_{\mathrm{Pre}} + OC_{HP} + OC_{BP} + OC_{VP} + OC_{\mathrm{Steam}}) \times 365 \quad (50)$$

- RO–PRO system:

$$OC_{\mathrm{Power}}[\$/y] = (OC_{IT} + OC_{\mathrm{Pre}} + OC_{HP} + OC_{BP} - OC_{\mathrm{Tur}}) \times 365 \quad (51)$$

- RO–MD–PRO system:

$$OC_{\mathrm{Power}}[\$/y] = (OC_{IT} + OC_{\mathrm{Pre}} + OC_{HP} + OC_{BP} + OC_{VP} + OC_{\mathrm{Steam}} - OC_{\mathrm{Tur}}) \times 365 \quad (52)$$

$$OC_{\mathrm{MR}}[\$/y] = CC_{\mathrm{Mem}} \times 0.2 \quad (53)$$

$$OC_{etc}[\$/y] = \text{AOC} \times 0.3 \quad (54)$$

$$\text{AOC}[\$/\text{y}] = \text{OC}_{power} + \text{OC}_{MR} + \text{OC}_{etc} \quad (55)$$

where OC_{power} is the annual power cost; OC_{MR} is the annual membrane replacement cost; and OC_{etc} is the labor, chemical, and maintenance cost. Finally, the water cost is as follows:

$$WC[\$/m^3] = (\text{ACC} + \text{AOC}) / (365 \times Q_p \times \text{PLF}) \quad (56)$$

2.6. Simulation conditions

In order to investigate the effect of hybridization between RO and MD and/or PRO, the economical evaluations were performed for 100,000 m³/d hybrid desalination plant. The values of model parameters and operating conditions used in this study are listed in Table 1. Basically, the value of model parameters and operating conditions was set that hybrid processes have price competitiveness than RO process.

3. Results and discussion

3.1. Performance of the RO, RO–MD, RO–PRO, and RO–MD–PRO systems

The performance of the RO, RO–MD, RO–PRO, and RO–MD–PRO systems was simulated under the given conditions in Table 1 and the results were summarized in Table 2. In the RO plant, the flux was 12.0 LMH and the permeate concentration was 370 mg/L. The specific energy and water cost were 3.32 kWh/m³ and 1.026 USD/m³, respectively. In this study, the electricity cost was set relatively high (0.2 USD/kWh), therefore, the water cost of RO plant system was estimated to be over 1.0 USD per unit volume. In the RO–MD hybrid plant, because the concentrated RO brine is used as the MD feed solution, the recovery of water increased from 40% to 58% and the brine flow rate also decreased from 150,000 to 72,400 m³/d. Nevertheless, the brine TDS increased from 71,400 to 102,000 mg/L. In the RO–MD hybrid plant, the permeate TDS decreased from 370 to 255 mg/L due to high ion rejection by MD. The specific energy, thermal energy, and water cost were calculated to 2.80 kWh/m³, 1,208,000 kW and 0.861 USD/m³, respectively. With the same production capacity (100,000 m³/d) condition to RO plant, the water cost of RO–MD plant decreased down by approximately 16%, because the sum of the operating cost of RO plant is much higher than the sum of the operating cost of RO–MD hybrid plant due to low specific energy and steam cost.

In the RO–PRO hybrid plant, the specific energy consumption decreased from 3.32 to 2.68 kWh/m³. This is because the brine from the RO process is used as a draw solution for the PRO process and pretreated effluent from a wastewater treatment plant is used as the feed solution for the PRO process. In addition, the water cost was calculated to 1.017 USD/m³. In the RO–PRO hybrid plant, the operating cost decreased due to lower specific energy consumption but the capital cost increased due to the additional PRO process. Although the brine flow rate increased from 150,000 to 250,000 m³/d, the brine concentration was decreased from 71,400 to 47,700 mg/L. Accordingly, it is expected that RO–PRO hybrid plant can alleviate the disposal and environmental problems of waste RO brine.

In the RO–MD–PRO hybrid plant, the recovery of water increased from 40% to 58% and the brine TDS also decreased from 71,400 to 58,000 m³/d compared with RO plant under similar brine flow rate. This is attributed to the fact that the RO brine is used as the MD feed solution and then MD brine is used as a draw solution for the PRO process. Accordingly, it is likely that the RO–MD–PRO hybrid plant is the most

Table 1
Parameters and operating conditions for simulations

	Parameter	Value
RO	Feed TDS	43,000 mg/L
	Recovery	40%
	Membrane area	40 m²
	Module per vessel	7
	Water permeability	2.2×10^{-12} m/s Pa
	Salt permeability	2.0×10^{-8} m/s
	Feed pressure	66.67 bar
	Pump efficiency	75%
	ERD efficiency	95
MD	Feedwater	RO brine
	Recovery	30%
	Membrane area	7.6 m²
	Module per vessel	1
	Pore size	0.1 μm
	Porosity	80%
	Tortuosity	2.5
	Membrane thickness	200 μm
	Module length	0.4 m
	Salt permeability	2.0×10^{-8} m/s
	Feed temperature	80°C
	Vacuum pressure	0.1 bar
	ERD efficiency	95
PRO	Feedwater	RO/RO–MD brine
	Recovery	167.7%
	Membrane area	20 m²
	Module per vessel	2
	Water permeability	7.0×10^{-12} m/s Pa
	Salt permeability	1.2×10^{-8} m/s
	ICP resistance	4.5×10^{5} s/m
Cost	Electricity bill	0.2 $/kWh
	Steam cost	0.15 $/ton
	Membrane cost	20 $/m²
	Plant load factor	0.91
	Interest rate	3%
	Plant life	20 years
	Plant load factor	0.91

effective to reduce environmental impacts of brine and water cost. The energy consumption was also reduced from 3.32 to 2.47 kWh/m^3 due to higher power density for PRO.

Fig. 2 shows the simulation results on the effect of feed TDS on the operation cost for the four desalination plants including RO, RO–MD, RO–PRO and RO–MD–PRO. The capacity was set to 100,000 m^3/d and the seawater TDS was adjusted from 35,000 to 44,000 mg/L. In this calculation, the parameters and operating condition except for seawater TDS are the same as those shown in Table 1. The change in seawater TDS affected the capital cost as changing cost of high-pressure pump, booster pump, and energy recovery device and operating cost as changing energy consumption. The simulation results showed that the water cost of RO, RO–MD, RO–PRO, and RO–PRO–MD plants ranged from 0.944 to 1.037 USD/m^3, from 0.800 to 0.860 USD/m^3, from 0.9617 to 1.025 USD/m^3 and from 0.830 to 0.865 USD/m^3 with the changes in the feed TDS, respectively.

The water cost of all plants increased with increasing seawater concentration because of an increase in energy consumption by the high-pressure pump to produce the same water flux in RO process. The water cost of RO plant is greatly influenced by the feed TDS because the electricity energy consumption of RO plant was the highest. On the other hand, the rates of water cost increase for RO–PRO and RO–MD–PRO plant were lower because the power density of PRO process also increased. This means that the feed TDS increased the energy consumption of RO process and the energy production of PRO process. In this calculation, the water cost of RO–MD and RO–MD–PRO hybrid plant were lower than RO plant under all feed TDS conditions and the difference in water cost between RO and two RO hybrid plant was getting larger as the feed TDS was increased. But the water cost of RO–PRO plant was higher than RO plant in the low TDS conditions, therefore, the feed TDS under these simulation conditions should exceed 40,000 mg/L to make the RO–PRO hybrid plant more price competitive than the RO plant.

Fig. 3 shows the simulation results for a 100,000 m^3/d of RO, RO–MD, RO–PRO, and RO–MD–PRO plant according to a change in electricity cost from 0.05 to 0.5 USD/kWh. In this calculation, the parameters and operating condition except for electricity cost are the same as those shown in Table 1. The

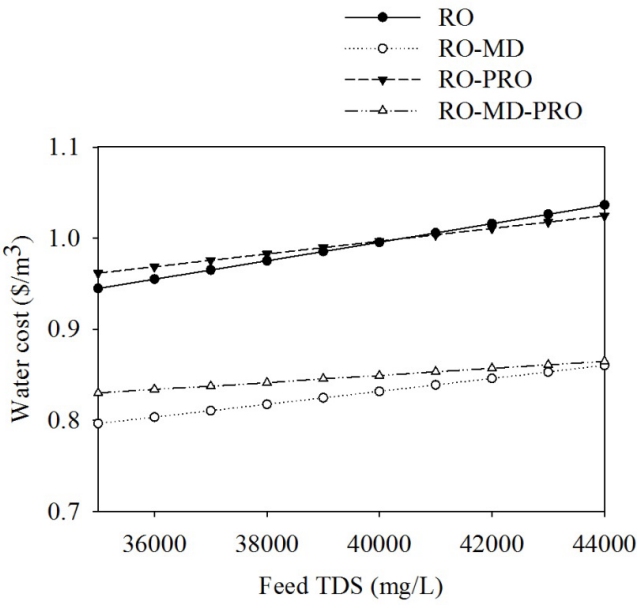

Fig. 2. The water cost estimation results according to a variation in seawater concentration.

Table 2
Simulation results of 100,000 m^3/d RO and RO hybrid plant

Parameter	RO	RO–MD	RO–PRO	RO–MD–PRO
Permeate (m^3/d)	100,000	100,000	100,000	100,000
Recovery (%)	40	58	40	58
Flux (LMH)	12	RO: 12 MD: 10	RO: 12 PRO: 14	RO: 12 MD: 10 PRO: 14
Power density (W/m^2)	–	–	10.2	15.5
Permeate TDS (mg/L)	370	255	370	255
Brine (m^3/d)	150,000	72,400	250,000	172,500
Feed TDS (mg/L)	43,000	43,000	43,000	43,000
Brine TDS (mg/L)	71,400	102,000	47,700	58,900
Specific energy (kWh/m^3)	3.32	2.80	2.68	2.47
Thermal energy (kW)	0	1,208,000	0	1,208,000
Annual capital cost ($/year)	5,000,200	5,300,210	7,556,800	6,410,700
Annual operating cost ($/year)	32,456,600	26,120,600	29,589,200	25,008,900
Water cost ($/m^3)	1.026	0.861	1.017	0.861

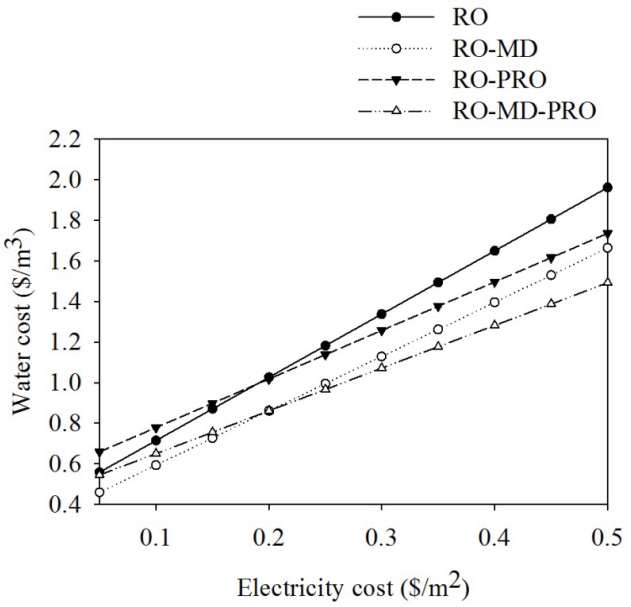

Fig. 3. The water cost estimation results according to a variation in electricity cost.

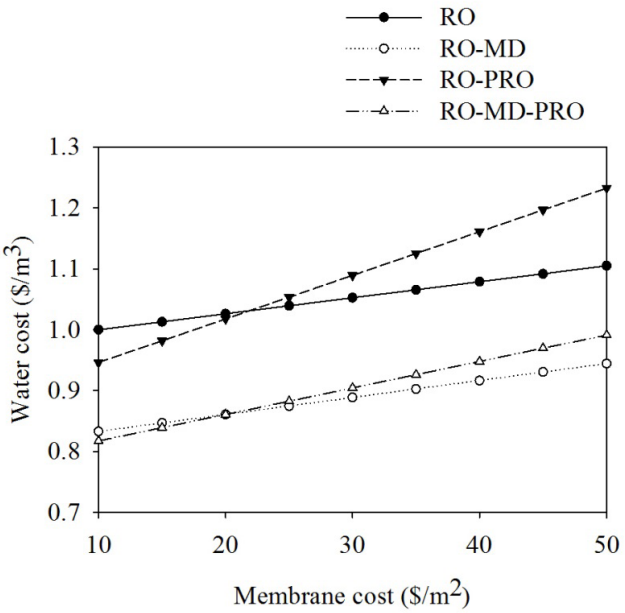

Fig. 4. The water cost estimation results according to a variation in membrane cost.

change in electricity cost affected only the operating cost as changing energy cost. The simulation results showed that the water cost of RO, RO–MD, RO–PRO, and RO–PRO–MD plant ranges from 0.559 to 1.961 USD/m^3, from 0.460 to 1.663 USD/m^3, from 0.659 to 1.736 USD/m^3, and from 0.545 to 1.493 USD/m^3 with the changes in the electricity cost, respectively.

As expected, the water cost of all plants was sensitive to the electricity cost. The water cost of RO plant was greatly influenced by the electricity cost because the energy consumption of RO plant was the highest, as shown in Table 2. In this calculation, since the steam cost was set to low, the water cost of RO–MD and RO–MD–PRO plant was lower than RO plant in all cases and the rate of water cost increase of RO–MD and RO–MD–PRO plant was lower than RO plant. To make the RO–PRO and RO-MD-PRO hybrid plant more price competitive than the RO plant, electricity cost under these simulation conditions should exceed 0.2 USD/kWh.

The simulation results for a 100,000 m^3/d RO, RO–MD, RO–PRO, and RO–MD–PRO plant according to a change in membrane cost from 10 to 50 USD/m^2 are shown Fig. 4. In this calculation, the parameters and operating condition except for membrane cost are the same as those shown in Table 1. The membrane cost was equally applied to RO, MD, and PRO membrane. The change in membrane cost affected the capital cost as changing total membrane cost, and operating cost as changing membrane replacement cost. The simulation results showed that the water cost of RO, RO–MD, RO–PRO, and RO–PRO–MD plant ranges from 1.000 to 1.105 USD/m^3, from 0.833 to 0.944 USD/m^3, from 0.946 to 1.233 USD/m^3, and from 0.817 to 0.991 USD/m^3 with the changes in the membrane cost, respectively. The change in membrane cost has the least effect on the RO plant but has the greatest effect on the RO–PRO plant because the total membrane area of RO plant was the smallest and the total membrane area of RO–PRO plant was the largest. To make the RO–PRO hybrid plant more price competitive than the RO plant, membrane

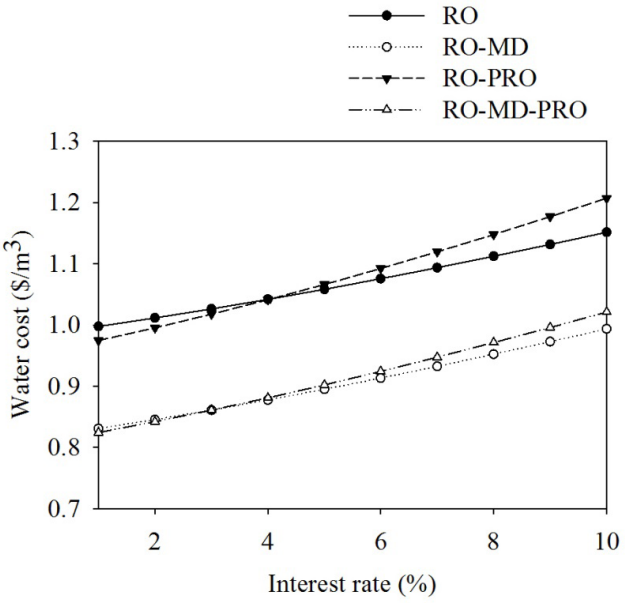

Fig. 5. The water cost estimation results according to a variation in interest rate.

cost under these simulation conditions should not exceed 0.22 USD/m^2.

In Fig. 5, the simulation results for a 100,000 m^3/d RO and hybrid plant according to a change in interest rate from 1% to 10% are presented. In this calculation, the parameters and operating condition except for interest rate are the same as those shown in Table 1. The change in interest rate affected only the capital cost as changing annual capital cost. The simulation results showed that the water cost of RO, RO–MD, RO–PRO, and RO–PRO–MD plant ranges from 1.000

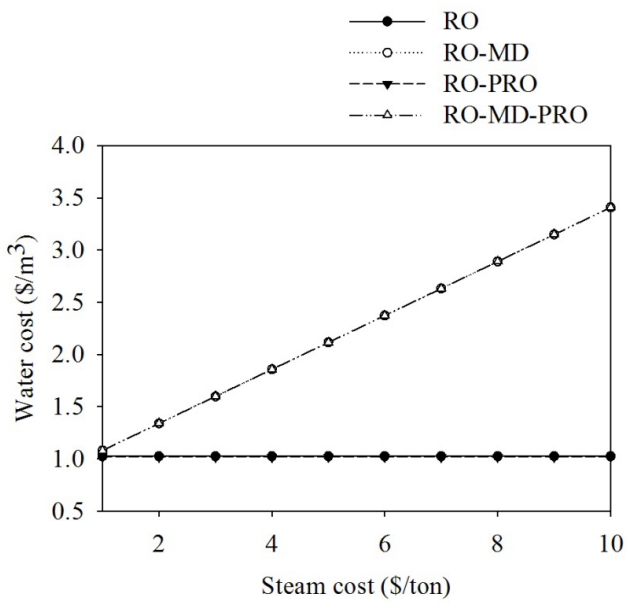

Fig. 6. The water cost estimation results according to a variation in steam cost.

to 1.15 USD/m^3, from 0.833 to 0.994 USD/m^3, from 0.975 to 1.201 USD/m^3, and from 0.824 to 1.021 USD/m^3 with the changes in the interest rate, respectively. The change in interest ratio has the greatest effect on the RO–PRO plant because the capital cost ratio to water cost is the highest.

Fig. 6 shows the simulation results for a 100,000 m^3/d RO and hybrid plants according to a change in steam cost for MD heat source from 0 to 10 USD/ton. In this calculation, the parameters and operating condition except for steam cost are the same as those shown in Table 1. The change in steam cost affected only the operating cost of MD process as changing power cost. In the MD process, the total power cost was the sum of the total electricity cost and total thermal energy cost.

The simulation results showed that the water cost of RO–MD and RO–PRO–MD plant ranges from 0.822 to 3.408 USD/m^3, from 0.822 to 3.408 USD/m^3 with the changes in the steam cost, respectively. The water cost of RO and RO–PRO plant was 1.026 and 1.017 USD/m^3, respectively. The simulation result shows that in hybrid process containing MD, the steam cost is most important cost parameter. The steam cost ratio to water cost is very high; the water cost of RO–MD and RO–MD–PRO was almost same according to the variation of steam cost. To make the RO–MD and RO–MD–PRO hybrid plant more price competitive than the RO plant, steam cost under these simulation conditions should not exceed 0.15 USD/kWh. This means that the hybrid desalination plant containing MD system should use free waste heat to gain price competitive advantage.

4. Conclusions

In this study, the performance and economic evaluation of RO–MD, RO–PRO, and RO–MD–PRO hybrid processes were carried out to identify key factors affecting their cost-effectiveness. The following conclusions can be drawn from this work:

- The RO–MD–PRO hybrid plant can give the most effective result since it allows the lowest water cost as well as the environmental impact by the brine. The other hybrid systems are also better than the RO stand-alone system in terms of water cost and brine problem.
- The electricity cost plays a dominant role in determining economic feasibility of the hybrid plants. At high electricity cost, the hybrid plants gain a competitive advantage over the RO stand-alone system. The water costs of RO–MD and RO–MD–PRO hybrid systems were sensitive to the steam cost for MD heating source.
- The feed TDS, membrane cost, and interest rate are also crucial factors in determining economic feasibility of hybrid systems.

Acknowledgment

This research was supported by a grant (code 16IFIP-B065893-04) and a grant (16FIP-B116951-01) from Industrial Facilities & Infrastructure Research Program funded by Ministry of Land, Infrastructure and Transport of Korean government.

References

[1] Human Development Report 2006 – Beyond Scarcity: Power, Poverty and the Global Water Crisis (2006). UNDP Human Development Reports (2006).
[2] S. Sadri, M. Ameri, R.H. Khoshkhoo, Multi-objective optimization of MED-TVC-RO hybrid desalination system based on the irreversibility concept, Desalination, 402 (2017) 97–108.
[3] C. Fritzmann, J. Löwenberg, T. Wintgens, T. Melin, State-of-the-art of reverse osmosis, Desalination, 216 (2007) 1–76.
[4] R. Rautenbach, T. Linn, D.M.K. Al-Gobaisi, Present and future pretreatment concepts-strategies for reliable and low-maintenance reverse osmosis seawater desalination, Desalination, 110 (1997) 97–106.
[5] P. Sukitpaneenit, T.-S. Chung, High performance thin-film composite forward osmosis hollow fiber membranes with macrovoid-free and highly porous structure for sustainable water production, Environ. Sci. Technol., 46 (2012) 7358–7365.
[6] J.R. McCutcheon, R.L. McGinnis, M. Elimelech, Desalination by ammonia–carbon dioxide forward osmosis: influence of draw and feed solution concentrations on process performance, J. Membr. Sci., 278 (2006) 114–123.
[7] N. Ghaffour, T.M. Missimer, G.L. Amy, Technical review and evaluation of the economics of water desalination: current and future challenges for better water supply sustainability, Desalination, 309 (2013) 197–207.
[8] S. Lattemann, T. Höpner, Environmental impact and impact assessment of seawater desalination, Desalination, 220 (2008) 1–15.
[9] K.W. Lawson, D.R. Lloyd, Membrane distillation, J. Membr. Sci., 124 (1997) 1–25.
[10] A.M. Alklaibi, N. Lior, Membrane-distillation desalination: status and potential, Desalination, 171 (2005) 111–131.
[11] L. Mariah, C.A. Buckley, C.J. Brouckaert, E. Curcio, E. Drioli, D. Jaganyi, D. Ramjugernath, Membrane distillation of concentrated brines—role of water activities in the evaluation of driving force, J. Membr. Sci., 280 (2006) 937–947.
[12] C.R. Martinetti, A.E. Childress, T.Y. Cath, High recovery of concentrated RO brines using forward osmosis and membrane distillation, J. Membr. Sci., 331 (2009) 31–39.
[13] L.D. Banchik, M.H. Sharqawy, J.H. Lienhard V, Limits of power production due to finite membrane area in pressure retarded osmosis, J. Membr. Sci., 468 (2014) 81–89.
[14] F. Helfer, C. Lemckert, Y.G. Anissimov, Osmotic power with pressure retarded osmosis: theory, performance and trends-a review, J. Membr. Sci., 453 (2014) 337–358.

[15] T. Thorsen, T. Holt, The potential for power production from salinity gradients by pressure retarded osmosis, J. Membr. Sci., 335 (2009) 103–110.
[16] C.F. Wan, T.-S. Chung, Osmotic power generation by pressure retarded osmosis using seawater brine as the draw solution and wastewater retentate as the feed, J. Membr. Sci., 479 (2015) 148–158.
[17] S. Lee, R.M. Lueptow, Membrane rejection of nitrogen compounds, Environ. Sci. Technol., 35 (2001) 3008–3018.
[18] J.I. Mengual, L. Pena, Membrane distillation, Colloids Surf., B, 1 (1997) 17–29.
[19] R.W.A. Schofield, A.G. Fane, C.J.D. Fell, Heat and mass transfer in membrane distillation, J. Membr. Sci., 33 (1987) 299–313.
[20] H.M. Sharqawy, H.L.V. John, M.Z. Syed, Thermophysical properties of seawater: a review of existing correlations and data, Desal. Wat. Treat., 16 (2010) 354–380.
[21] M. Khayet, M.P. Godino, J.I. Mengual, Theory and experiments on sweeping gas membrane distillation, J. Membr. Sci., 165 (2000) 261–272.
[22] M. Khayet, M.P. Godino, J.I. Mengual, Nature of flow on sweeping gas membrane distillation, J. Membr. Sci., 170 (2000) 243–255.
[23] J.I. Mengual, M. Khayet, M.P. Godino, Heat and mass transfer in vacuum membrane distillation, Int. J. Heat Mass Transfer, 47 (2004) 865–875.
[24] M.A. Darwish, M. Abdel-Jawad, G.S. Aly, Technical and economical comparison between large capacity multi stage flash and reverse osmosis desalting plants, Desalination, 72 (1989) 367–379.
[25] Y. Dreyzin, Ashkelon seawater desalination project-Off-taker's self costs, supplied water costs and benefits, Desalination, 190 (2006) 104–116.
[26] C. Sommariva, Desalination Management and Economics, Mott Mac Donald, Faversham House Group, Surrey, 2004.
[27] A. Malek, M.N.A. Hawlader, J.C. Ho, Design and economics of RO seawater desalination, Desalination, 105 (1996) 245–261.
[28] M.G. Marcovecchio, P.A. Aguirre, N.J. Scenna, Global optimal design of reverse osmosis networks for seawater desalination: modeling and algorithm, Desalination, 184 (2005) 259–271.
[29] F. Marechal, E. Aoustin, P. Bréant, Multi-objective optimization of RO desalination plants, Desalination, 222 (2008) 96–118.